Biointerphases (2012) 7:52
DOI 10.1007/s13758-012-0052-8

Epidermal Differential Impedance Sensor for Conformal Skin Hydration Monitoring

Xian Huang · Woon-Hong Yeo · Yuhao Liu · John A. Rogers

Received: 22 June 2012 / Accepted: 2 August 2012

Abstract We present the design and use of an ultrathin, stretchable sensor system capable of conformal lamination onto the skin, for precision measurement and spatial mapping of levels of hydration. This device, which we refer to as a class of 'epidermal electronics' due to its 'skin-like' construction and mode of intimate integration with the body, contains miniaturized arrays of impedance-measurement electrodes arranged in a differential configuration to compensate for common-mode disturbances. Experimental results obtained with different frequencies and sensor geometries demonstrate excellent precision and accuracy, as benchmarked against conventional, commercial devices. The reversible, non-invasive soft contact of this device with the skin makes its operation appealing for applications ranging from skin care, to athletic monitoring to health/wellness assessment.

1 Introduction

Skin hydration monitoring is a well-established and important technique in dermatology, for analyzing various diseases and determining the effectiveness of medical therapies [1–4]. Hydration measurement is also useful in cosmetology, for assessing the function of anti-aging and moisturization treatments [5–8]. Skin hydration levels are typically characterized by measurements of skin electrical impedance [9–12] or thermal conductivity [13], or by optical spectroscopic techniques [9, 14, 15] including reflectivity [16]. Indirect methods include evaluation of mechanical properties of the skin [17–19] or its surface geometry [20, 21]. Among these methods, electrical impedance provides the most reliable and established assessment, due to its instrumental simplicity and minimized cost. Several commercial systems that perform this measurement are available [22–25]. Such technologies generally rely on physical contact between the soft, curved surface of the skin, and rigid, planar electrodes [22]. Here, the accuracy and repeatability both depend critically on the contact force between the electrodes and the skin. As a result, most devices incorporate pressure-sensing components that help the user to apply, with precision, the appropriate force during measurement. Such devices are not well suited for spatial mapping, for evaluating sensitive areas of the skin, or for continuous monitoring, thereby greatly limiting their utility [26].

Here we present a different approach, based on extensions of previously reported concepts in 'epidermal' electronics, in which semiconductor and related devices mount on ultrathin, elastomeric sheets in open mesh geometries, and integrate with the skin in a soft, van der Waals process, without any external application of pressure. This process achieves intimate biotic/abiotic contact in a way that does not mechanically load or constrain the natural motions of the skin [27]. When incorporating devices with multiple functions, these epidermal systems enable non-invasive detection of physiological parameters such as electrical signals associated with activity in the brain, heart and skeletal muscles. In the following, we describe ideas and demonstration examples for an epidermal class of differential hydration sensor based on electrical impedance detection. The sensors effectively eliminate requirements

This article is part of the Topical Collection "In Focus: Future of Biosensors".

X. Huang · W.-H. Yeo · Y. Liu · J. A. Rogers (✉)
Frederick Seitz Materials Research Laboratory, Department of Materials Science and Engineering, University of Illinois at Urbana-Champaign, Urbana, IL 61801, USA
e-mail: jrogers@illinois.edu

Published online: 23 August 2012

on precise, external control of contact force, in a mode of integration that is mechanically 'invisible' to the wearer. The measurement outcomes can be interpreted using conventional approaches for impedance evaluation [28, 29]. The experimental results demonstrate, in fact, precision and accuracy that compare favorably to commercial moisture meters (CMM). Differential sensing schemes can be incorporated naturally, to compensate for variations in temperature, stresses/strains associated with human activity, and other disturbances that may lead to unexpected impedance changes. This capability is particularly valuable for applications in continuous monitoring. Arrays of miniaturized sensors can be achieved, for spatial mapping and, potentially, depth profiling of hydration. These collective attributes suggest that this type of technology, particularly when combined with other classes of sensors in a single system, could be valuable for wide-ranging uses in human healthcare and wellness evaluation.

2 Principle and Sensor Design

The epidermal hydration measurements reported here use impedance measurements performed directly on the skin, to exploit known correlations between electrical parameters of biological tissues and their water content [30]. In particular, both the conductivity and permittivity of human skin change with the skin hydration levels [25, 30]. As a result, the hydration levels can be determined through impedance measurements, through appropriate calibration.

2.1 Epidermal Skin Hydration Sensor with Differential Detection

Figure 1 shows images and schematic illustrations of an epidermal skin hydration sensor platform that consists of pairs of electrodes designed to quantify skin impedance. These electrodes form eight separate measurement channels (Fig. 1a, labels 1 through 8), all with a common electrical ground. Channels 1 through 4 directly contact the skin, while 5 through 8 are insulated from it by thin layers of dielectric with embedded electrodes as floating grounds. We refer to the former (i.e. channels 1–4) and latter (i.e. channels 5–8) as measuring and reference electrodes, respectively. Figure 1e provides a cross sectional illustration of a representative pair. Electrodes on common rows have identical geometries and designs: meander (Fig. 1a; top row), interdigitated (Fig. 1a; middle row), and circular (Fig. 1a; bottom row) electrodes. Figure 1b shows a magnified view of the last case, with reference and measuring electrodes on the left and right, respectively. The electrodes terminate at bonding pads near the edge of the overall system, joined through interconnects with serpentine geometries in mesh layouts that incorporate square pads at the nodes. Differential detection enabled by combined use of measuring and reference electrodes allows rejection of common mode disturbances in the measurement system as well as impedance changes caused by deformations in the serpentine interconnections.

The fabrication of this device involves first spin-coating a sacrificial layer of polymethylmethacrylate (PMMA; 500 nm thick) and a layer of polymide (PI; 1 μm thick) on a silicon (Si) wafer substrate. Photolithographically patterned layers of Cr (5 nm) and Au (400 nm) form the electrodes as well as the serpentine interconnections, both of which include a top coating of PI (1 μm). Reactive ion etching (RIE) through selected regions of the PI defines vias to allow subsequent metallization to contact the serpentine interconnect traces at well-defined points. An additional patterned bilayer of Cr/Au (5 nm/200 nm) forms the floating ground plates. A final, uniform coating of PI (1 μm) encapsulates the system. Patterned RIE through the entire multilayer stack creates openings to allow contact with the skin and the open mesh structures needed to achieve desired levels of mechanical deformability. Removing the underlying PMMA by immersion in acetone for 5 min at 100 °C, allows the mesh to be removed from the Si wafer by use of water-soluble poly(vinylalcohol) (PVA) tape (Wave Solder Tape 5414, 3M Co.). Layers of Ti/SiO_2 (5/40 nm) evaporated onto the backside of the released structure facilitate bonding to a thin, low-modulus silicone substrate (Solaris, Smooth-On, Inc.), first activated by treatment with ultraviolet induced ozone (10 min) to create reactive hydroxyl functionality on the surface. Dissolving the PVA tape in water for 20 min completes the fabrication, resulting in a mechanical construction that affords excellent stretchability (Fig. 1c) and flexibility (Fig. 1d), with a low effective modulus, which are all requirements for epidermal integration.

2.2 Conformal Skin Contact of the Hydration Sensor

The mechanics of the epidermal hydration sensor enable its integration with skin in a dry, physical lamination process, driven only by van der Waals interactions [27]. The result offers a reversible, conformal contact, in a thin and highly compliant configuration that allows the system to accommodate natural motions of the skin without delamination. This mode of integration not only forms a robust mechanical interface, but also a reproducible electrical contact to the skin, for the purpose of precise and reproducible impedance measurements. Figure 2a shows a device mounted on skin, in an undeformed state. The silicone substrate in this case is only 5 μm thick; mounting involves applying the device to the skin using a temporary, water-soluble film of PVA for handling [27]. The device

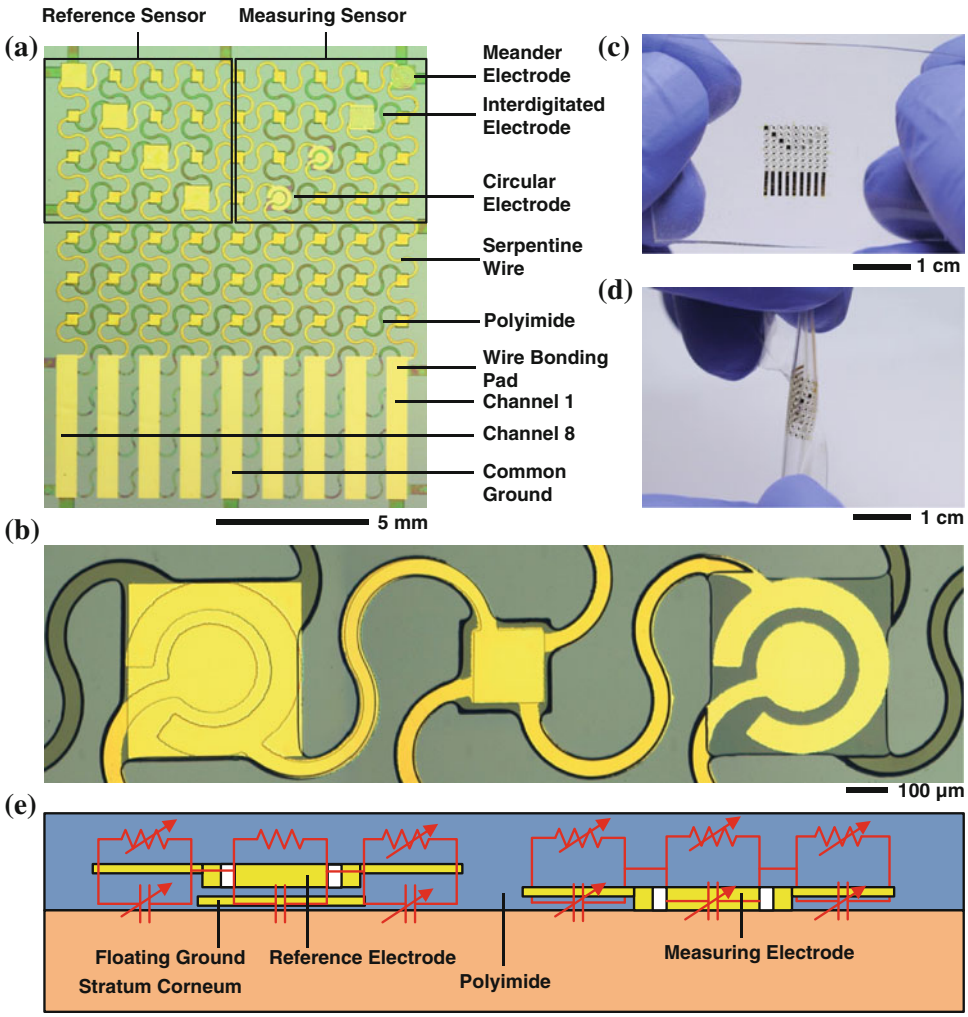

Fig. 1 Schematic illustrations and images of a differential hydration sensor platform with epidermal construction. **a** Optical micrograph showing the electrode layout for a representative device on a silicon wafer just before transfer to a thin, silicone substrate. **b** Optical micrograph of a pair of reference (*left*) and measuring (*right*) electrodes, with concentric designs, corresponding to channels 4 and 5 in **a**. Images of a device during **c** uniaxial stretching and **d** twisting. **e** Schematic illustration and equivalent circuit model (*red*) of a reference (*left*) and measuring (*right*) electrode

stretches with the skin, in a manner that does not impose any significant mechanical constraints, as shown for the case of various deformations (Fig. 2b–e). Devices with somewhat thicker substrates (e.g. 50–100 μm) offer similarly favorable mechanics but with sufficient physical toughness to allow manual peeling from and re-attachment to the skin, for repeated use (Fig. 2f).

3 Experimental Setup and Methods

3.1 Epidermal Differential Hydration Sensor

The sensors exploit three different designs. The circular electrodes involve a concentric design (Fig. 1b), consisting of inner disks (150 or 125 μm in radius) surrounding by open-ended rings (inner radius: 200 μm, outer radius: 300 μm). The interdigitated electrodes incorporate 8 (upper digit) or 7 (bottom digit) fingers each with dimensions of 20 × 50 μm^2 and spacings of 20 μm. The meander electrodes involve two sets of four semicircular lines (radii: 30, 90, 150, and 210 μm, width: 20 μm) and two 60° and 150° arc lines (radii: 310 and 270 μm, width: 20 μm) interconnected into spiral shapes. In each of these three cases, the electrodes connect to corresponding bonding pads (width: 500 μm, spacing: 500 μm) and a common ground pad through serpentine traces (width 50 μm; ∼225 μm radii of curvature). The floating ground plates consists of 600 × 600 μm^2 pads situated above the reference electrodes and connected with serpentine traces through vias in the PI (230 × 230 μm^2 in dimension). The use of different electrode designs in a single device allows us to assess various hydration sensing methods and sensor parameters under the same experimental conditions. The meander electrodes perform as resistors, which can be used for assessment of skin hydration through purely resistivity measurement. The other electrodes measure both resistance and capacitance changes. The circular electrodes offer symmetries that facilitate theoretical analysis; these geometries are also found in macroscale electrodes used in CMM [22, 23], to enable direct comparison.

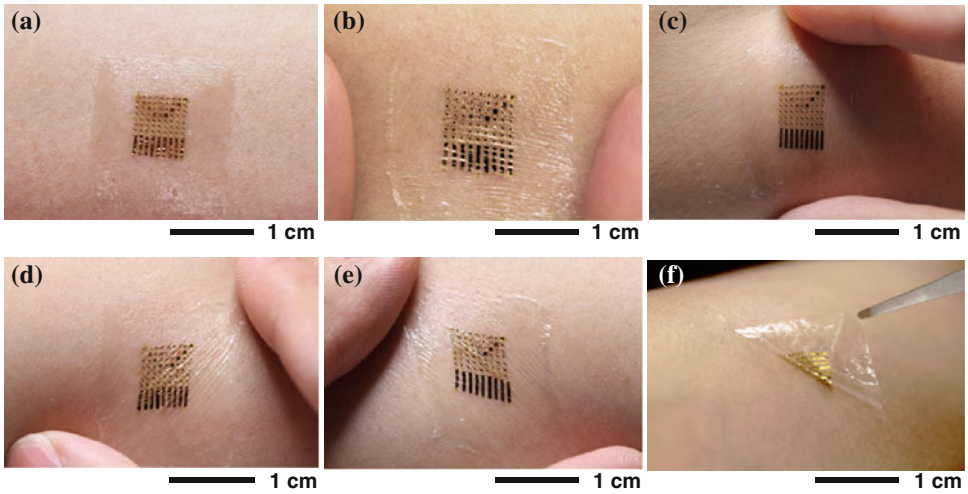

Fig. 2 Epidermal, differential hydration sensor systems mounted on the skin of the forearm. This sequence of images shows the device, undeformed (**a**), and uniaxially stretched along the horizontal (**b**), vertical (**c**), diagonal right (**d**) and diagonal left (**e**) directions. Here, the device adheres to the skin by van der Waals interactions alone, thereby allowing it to be easily peeled from the skin using tweezers (**f**)

3.2 Releasable, Stretchable Connector

Soft, stretchable and releasable connectors provide electrical interfaces between the hydration sensor systems and external impedance data acquisition (DAQ) hardware (Fig. 3a). The epidermal sensor can be connected directly to the DAQ by an anisotropic conductive film (ACF) cable. However, soft, stretchable connectors that allow releasable contact to the sensor provide advantages in re-use and they also lead to reduced stresses/strains on the sensor. The fabrication involves processes similar to those for the sensors, to yield connectors with nine conducting Au traces (thickness: 600 nm, width: 500 μm) in serpentine layouts and with spacings (500 μm) that match the bonding pads on the sensor systems. This construction, when used with a thin silicone substrate (thickness $\sim$100 μm), yields mechanical properties that are similar to those of the sensor (Fig. 3b, c). The connector interfaces with the DAQ through an ACF cable and with the hydration sensor through a releasable bond established by physical lamination (similar to that between the sensor and the skin) (Fig. 3d). This scheme provides a robust interface between the skin/hydration sensor and the ACF/DAQ, with no adverse effect on the contact of the sensor to the skin. In this scheme, the connector can be applied and removed, as necessary.

3.3 Multiplexing Impedance Analyzer for Hydration Measurement

An impedance analyzer circuit equipped with multiplexing measurement capability serves as a system for quantifying the response of the sensors (Fig. 3e). Here, an impedance analyzer chip (AD5933, Analog Devices) with a 12-bit resolution provides an alternating current (AC) voltage (V_{in}) (2 V peak to peak) at frequencies between 1 and 100 kHz to each channel of the hydration sensor through a multiplexer (ADG 708, Analog Devices). Changing the combination of voltages supplied to channel selecting pins in the multiplexer through an I/O controller (USB-8451, National Instruments) and a computer allows each individual sensor channel to be probed at a given value of V_{in}. The amplitude and phase of the output voltage (V_{out}) measured from the common ground changes with the electrical properties of the skin. The values of V_{out} from all sensor channels can be obtained in a time-sequence, and converted back to impedances within the impedance analyzer.

3.4 Experimental Methods and Materials

Experimental evaluations involve attaching (and removing) epidermal hydration sensor systems to the skin of the ventral forearm to reveal frequency dependent changes in impedance associated with application of moisturizing lotions (Intensive Rescue Moisture Body Lotion, Vaseline Inc.). Hydration measurements performed at frequencies where changes in impedance are maximized provide optimal sensitivity. A CMM (MoistureMeterSC Compact, Delfin Inc) [22] that is based on impedance measurement enables calibrated conversion of impedance measurements to hydration levels.

4 Results and Discussion

4.1 Frequency-Dependent Impedance Changes with Hydration Levels

The amplitude and phase of the impedances measured at each of the sensor channels change monotonically with the level of skin hydration, throughout the radio frequency (RF) range from 15 to 95 kHz. Representative responses appear in Fig. 4a, b for the case of channel 4. As the hydration levels changes from 31 to 110 (arb units from the CMM), the impedance amplitude decreases steadily by

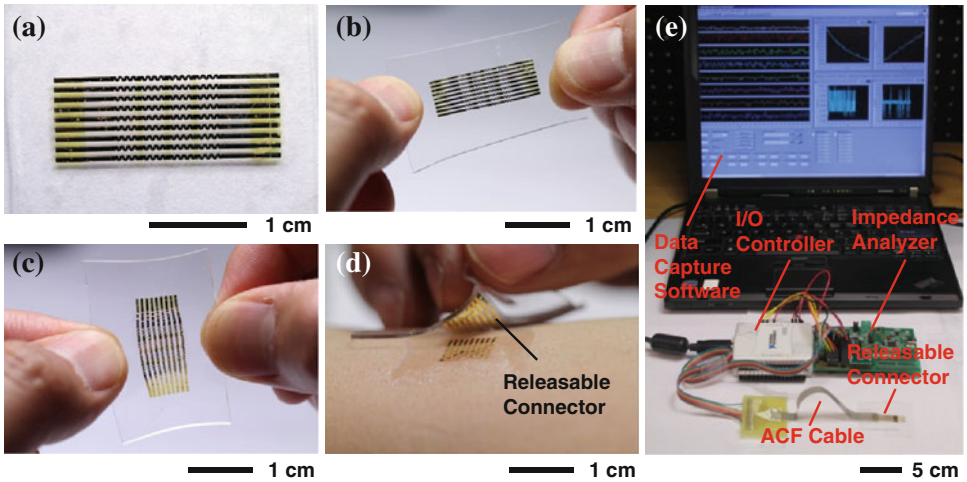

Fig. 3 Soft, releasable connectors provide interfaces between epidermal, differential hydration sensors and external data acquisition hardware. Images of a representative connector that uses a serpentine layout and a thin silicone substrate, in an **a** underformed configuration, and in states of uniaxial deformation parallel **b** and perpendicular **c** to its long dimension. The spacings of the traces match those of the bonding pads at the edge of the hydration sensor. The compliant, stretchable nature of the connector and the sensor allows reversible electrical contact between the two by physical lamination **d**. **e** Image of data acquisition hardware: an impedance analyzer, an I/O controller, a custom package of data capture software with graphical user interface, and an ACF cable between a printed circuit board and the releasable connector

$\sim$1.6 MΩ, while the impedance phase shifts by $\sim$1.18 rad. Furthermore, at a fixed hydration level of 90, the impedance amplitude decreases from 558 kΩ at 15 kHz to 332 kΩ at 95 kHz, while the phase increases by 0.36 rad over this same RF range. These trends arise from the frequency dependence of the conductivity and permittivity of the skin due mostly to expected effects in aqueous electrolyte solutions [31–34]. The result is increased changes in impedance with hydration levels at low measurement frequencies (e.g. 15 kHz). (We note that the noise near 60 kHz arises from harmonics in the power lines. Such effects can be eliminated either with appropriate notch filters [35, 36] or with batteries as power sources.)

Figure 4c, d show changes in impedance amplitude and phase with skin hydration levels at selected frequencies. As the hydration increases, the skin conductivity and permittivity both increase, leading to a decrease in the real part (resistive part) and the imaginary part (capacitive part) of the complex impedance. The magnitudes of these changes diminish with increasing frequencies: for the range studied, the impedance amplitude and phase change by 89 and 73 %, respectively, at 15 kHz and by 34 and 38 %, respectively, at 95 kHz. The highest sensitivity is, therefore, obtained at low frequencies in this RF range.

Similar impedance responses to hydration changes (as Fig. 4a, b) appear in other measuring channels (channel 1–3). As the hydration changes from 40 to 110, the impedances (at 15 kHz) of the meander electrode in channel 1 and the interdigitated electrode in channel 2 change from 255 to 24 Ω and from 2.54 to 2.52 MΩ, respectively. The interdigitated electrodes in channel 2 provides a useful design for electrodes [23, 24, 37], but the complexity in the associated distribution of electrical field lines leads to complications in theoretical analysis [38]. The symmetric sensor geometry of channel 3 and 4 enables direct comparison to outputs from the CMM, which has similar electrode construction, and the symmetry facilitates analytical modeling. For these reasons, the experimental results presented in the following focus on circular electrodes. In all cases, the impedance responses of the reference electrodes (channel 5–8) smaller than those of the measuring electrodes. In particular, the impedance changes (at 15 kHz) of the reference channels (from channel 5 to 8) are only 65, 31, 62, and 75 % of the changes in the corresponding measuring channels, and are likely due to electrical parasitic effects of the serpentine lines and passivated electrodes.

4.2 Comparison Between Hydration Measured by the CMM and Impedance Measured by the Epidermal Hydration Sensor

A calibration curve can convert the impedance measured by an epidermal hydration sensor to hydration levels measured by the CMM. One means to accomplish this calibration is to apply lotion to the skin and then to evaluate time dependent changes in the impedance and hydration levels. Figure 5a, c show results for the differences in the impedance amplitude and phase of channels 4 and 5 (Fig. 1b) and the output from the CMM. These experiments involve applying and then removing the devices at regular time intervals (5 s on skin and 2 min

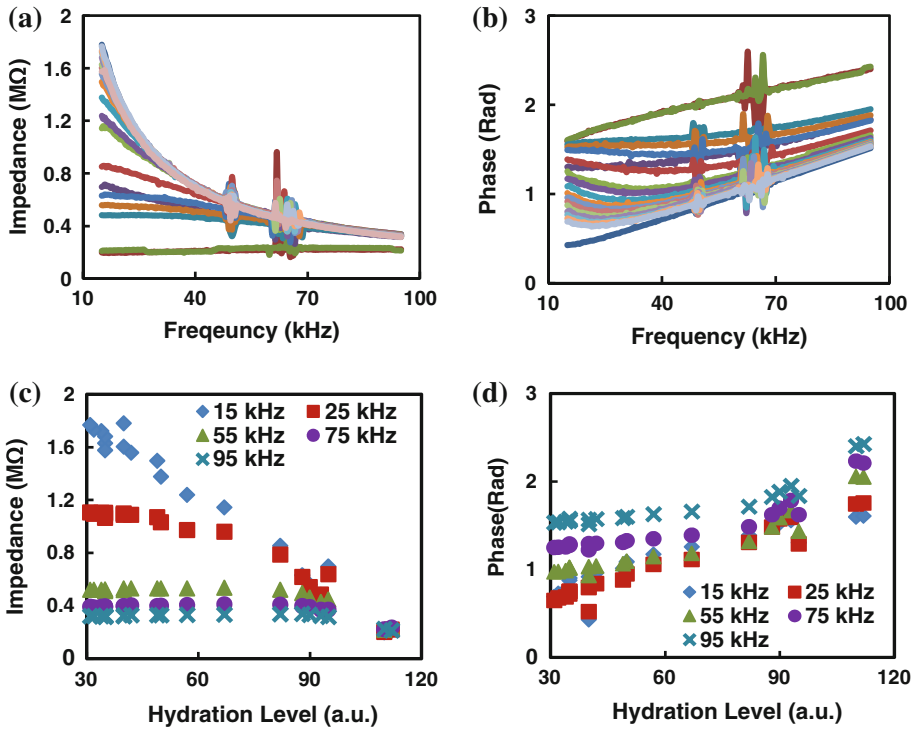

Fig. 4 Typical responses of epidermal hydration sensors to changes in skin hydration at frequencies from 15 to 90 kHz. Frequency dependent impedance **a** amplitude and **b** phase of channel 4 at various hydration levels. Hydration level dependent impedance **c** amplitude and **d** phase at selected measurement frequencies

between each application), to affect the measurements with minimal dwell times on the skin. The impedance of the channel 4 (measuring) changes systematically and significantly with skin hydration. By contrast, channel 5 (reference) shows minimal variation, likely due to some combination of small environmental changes, electrical parasitic effects of the serpentine lines, and/or physical deformations of the hydration sensor. The differential approach eliminates these contributions through the subtraction of the impedances of these two channels. The results indicate that the differential impedance amplitude and phase are inversely and directly proportional, respectively, to the hydration level. Specifically, as the CMM hydration level decreases from 110 to 22, the impedance amplitude increases from 25 to 48 kΩ. This trend is consistent with increased electrical conductivity and permittivity with increasing hydration [25, 30]. The former is expected because increased water content provides additional ionic pathways for charge transport. The latter is expected because the addition of water molecules increases the density of dipoles and also improves the flexibility of keratin in the stratum corneum, both of which enhance the ability of the skin to store electrical energy and respond more readily to applied electrical fields [39]. Given the monotonic correspondence between differential sensor impedance and hydration levels, the impedance values can be converted into hydration levels using a simple linear relationship, whose coefficients can be calculated using two reference hydration levels and the corresponding impedance values (amplitude and/or phase). The converted results shown in Fig. 5b, d exhibit excellent consistency with the CMM.

Using the same calibration method, experimental results, some of which appear in Fig. 4, can be converted into hydration levels using two reference values from the CMM (Fig. 6). The converted results after subtracting impedance amplitude difference between channel 4 and 5 as well as channel 3 and 6 exhibit excellent consistency between CMM and epidermal sensors. For example, over a measurement period of approximately 35 min, deviation between the hydration levels from the CMM and calibrated values from the epidermal sensor are <10 %.

4.3 Repeatability in Measurements of Hydration Using Epidermal Devices and CMM

Sequential steps of applying the device to the skin, performing a measurement and then removing the device can be used to determine the repeatability. In this process, the CMM must be delivered to the skin with carefully controlled force ranging from 1.37 to 2.06 N [22], enabled by readout from a built-in pressure sensor (Fig. 7a, c). By contrast, the epidermal hydration sensor interfaces to the skin by a soft, physical lamination process, in which van der Waals forces establish the contact without any externally applied force (Fig. 7b, d). This mode of operation,

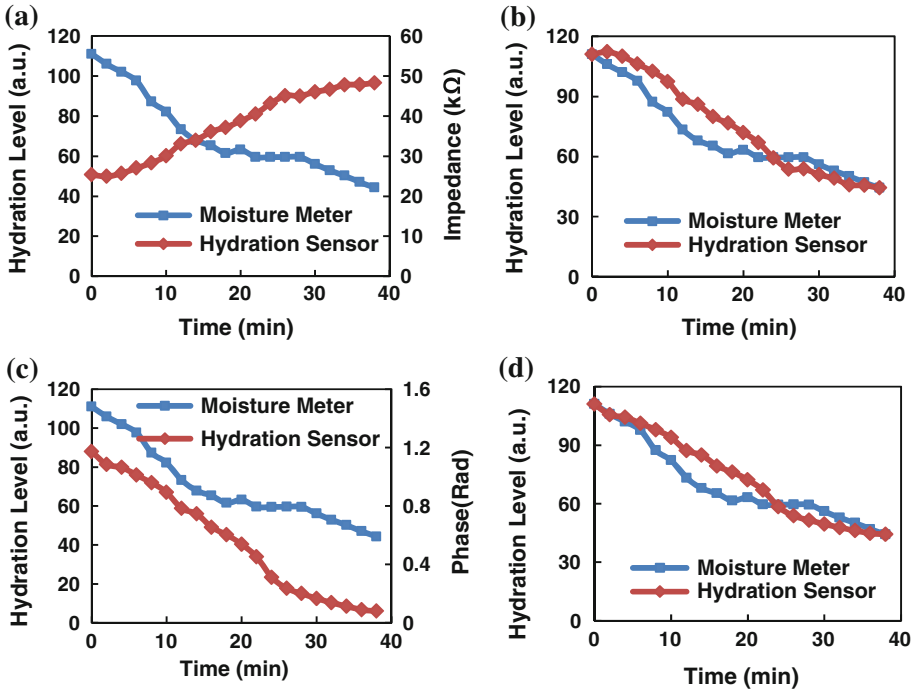

Fig. 5 Data that establish the relationships between hydration levels measured by a CMM and the differences in impedance amplitude and phase values measured by channels 4 (i.e. measuring) and 5 (i.e. reference) by an epidermal hydration sensor. The *left* frames **a**, **c** show the directly measured data; the *right* frames **b**, **d** show results after calibration

and the associated minimal mechanical pressure on and deformation of the skin, represent appealing attributes for practical applications. The results of ten measurements (Fig. 7e) indicate that the repeatability of the epidermal hydration sensor and the CMM are similar. The hydration levels measured by the epidermal sensor are stable at approximately 28.15 with a standard deviation of 0.74, while the CMM shows an average value of 28.28 and a standard deviation of 0.68. We note that the CMM, when used without careful attention to the pressure sensor, offers significantly worse repeatability than that indicated by the data of Fig. 7e.

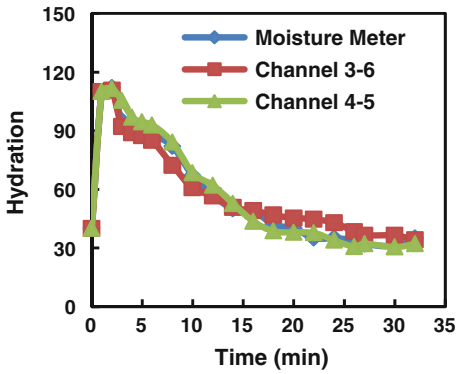

Fig. 6 Hydration levels measured by a differential epidermal hydration sensor calibrated by impedance amplitude difference and a CMM, over an extended period of time

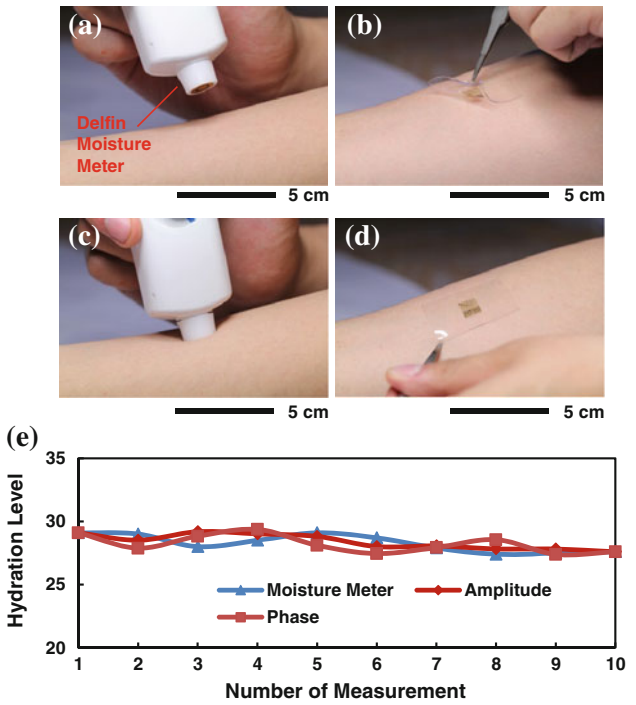

Fig. 7 Images and data corresponding to evaluations of repeatability in epidermal hydration sensors and CMMs. Images of a CMM placed adjacent to **a** and in contact with **c** the skin of the forearm. Images of an epidermal hydration sensor partially peeled-off **b** and attached to **d** a similar region of skin. **e** Data from the epidermal hydration sensor and the CMM for a sequential set of ten measurements, each involving application and removal of the device from the skin

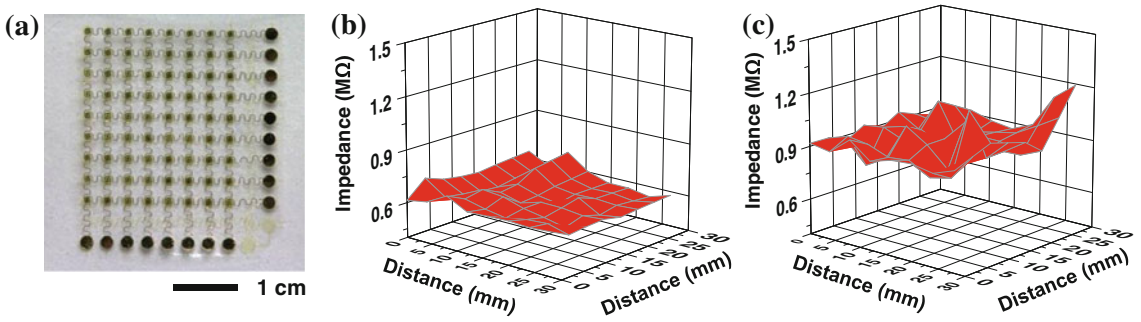

Fig. 8 Spatial mapping device used for large area hydration sensing. **a** A image of the spatial mapping hydration sensor with 8 × 8 electrode arrays. The hydration mapping result of skin at hydration levels of **b** 89 and **c** 45

4.4 Spatial Mapping of Hydration Levels

In addition to the advantages of soft contact to the skin, the epidermal device construction enables spatial mapping of hydration, at high levels of resolution through the addition of measuring sensors. A hydration sensor with an 8 × 8 array of circular electrode pairs (inner disks 200 μm in radius, outer rings 300 μm in inner radius and 450 μm in outer radius) demonstrates this capability, through measurement of hydration over a 3 × 3 cm^2 area of skin at a spatial resolution of 2 mm (Fig. 8a). Typical mapping results at two hydration levels appear in Fig. 8b, c. The spatial hydration sensor exhibited an average impedance of 0.62 MΩ at a fixed measurement frequency of 15 kHz at a hydration level of 89. With the decrease of hydration level to 45, the average impedance increased to 0.93 MΩ. The noise in impedance measurements is ∼1 % of the impedance level, suggesting that the impedance changes are mostly due to skin hydration variations, not limited by noise. This outcome is consistent with the relation between the impedance and skin hydration that we observed from differential hydration sensor, and indicates that this type of spatial mapping device has potential to be applied over large areas of the skin.

5 Conclusions

The results reported here illustrate a soft, 'skin-like' technology, capable of intimately and non-invasively integrating with the skin for the purpose of quantitative assessment of hydration levels. The accuracy and repeatability of the measurement are both comparable to conventional devices that rely on rigid electrodes and controlled pressures during contact with the skin. The ability to perform internally referenced detection, in a differential mode, and the straightforward scaling to arrays of sensors for spatial mapping applications represent two additional, valuable features. Development of silicone substrates with enhanced ability to accommodate skin transpiration, and incorporation of wireless data transmission capabilities represent important directions for future work.

Acknowledgments This work was carried out at the Fredrick Seitz Materials Research Laboratory Central Faciliteis, University of Illinois, which are partially supported by the US Department of Energy under grant DE-FG02-07ER46453 ad DE-FG02-07ER46471.

References

1. Blichmann C, Serup J (1987) Contact Dermat 16:155–159
2. Boguniewicz M, Nicol N, Kelsay K, Leung DYM (2008) Semin Cutan Med Surg 27:115–127
3. Sharma VM, Sridharan K, Pichan G, Panwar MR (1986) Ergonomics 29:791–799
4. Kleiner SM (1999) J Am Diet Assoc 99:200–206
5. Verdier-Sévrain S, Bonté F (2007) J Cosmet Dermatol 6:75–82
6. Zhang M, Mak AFT (1999) Prosthet Orthot Int 23:135–141
7. Choi JW, Kwon SH, Huh CH, Park KC, Youn SW (2012) Skin Res Technol 0:1–7
8. Gerhardt L-C, Strässle V, Lenz A, Spencer ND, Derler S (2008) J R Soc Interface 5:1317–1328
9. Frodin T, Helander P, Molin L, Skogh M (1988) Acta Derm Venereol 68:461–467
10. Tagami H, Ohi M, Iwatsuki K, Kanamaru Y, Yamada M, Ichijo B (1980) J Investig Dermatol 75:500–507
11. Paye M, Van de Gaer D, Morrison BM (1995) Skin Res Technol 1:123–127
12. Sasai S, Zhen Y-X, Tagami H (1996) Skin Res Technol 2:173–176
13. Xiao P, Ciortea LI, Singh H, Cui Y, Berg EP, Imhof RE (2010) J Phys: Conf Ser 214:012026
14. Attas EM, Sowa MG, Posthumus TB, Schattka BJ, Mantsch HH, Zhang SL (2002) Biopolymers 67:96–106
15. Kadlec F, Berta M, Kužel P, Lopot F, Polakovič V (2008) Phys Med Biol 53:7063–7071
16. Alekseev SI, Szabo I, Ziskin MC (2008) Skin Res Technol 14:390–396

17. Dobrev H (2000) Skin Res Technol 6:239–244
18. Hendriks FM, Brokken D, Oomens CWJ, Baaijens FPT (2004) Skin Res Technol 10:231–241
19. Xing L, Boppart SA (2010) IEEE Trans Biomed Eng 57:953–959
20. Hendriks FM (2005) Mechanical behaviour of human epidermal and dermal layers in vivo. Technische Universiteit Eindhoven
21. Tan G, Xu P, Lawson LB, He J, Freytag LC, Clements JD, John VT (2010) J Pharm Sci 99:730–740
22. Alanen E, Nuutinen J, Nicklén K, Lahtinen T, Mönkkönen J (2004) Skin Res Technol 10:32–37
23. Fluhr JW, Gloor M, Lazzerini S, Kleesz P, Grieshaber R, Berardesca E (1999) Skin Res Technol 5:161–170
24. Barel AO, Clarys P (1997) Skin Res Technol 3:107–113
25. Clarys P, Barel AO, Gabard B (1999) Skin Res Technol 5:14–20
26. Martinsen ØG, Grimnes S, Haug E (1999) Skin Res Technol 5:179–181
27. Kim D-H, Lu N, Ma R, Kim Y-S, Kim R-H, Wang S, Wu J, Won SM, Tao H, Islam A, Yu KJ, Chowdhury R, Ying M, Xu L, Li M, Chung H-J, Keum H, McCormick M, Liu P, Zhang Y-W, Omenetto FG, Huang Y, Coleman T, Rogers JA (2011) Science 333:838–843
28. Matthie JR (2008) Expert Rev Med Dev 5:239–261
29. Guimerà A, Calderón E, Los P, Christie AM (2008) Physiol Meas 29:S279–S790
30. Yamamoto T, Yamamoto Y (1976) Med Biol Eng Comput 14:151–158
31. Gabriel C, Gabriel S, Corthout E (1996) Phys Med Biol 41:2231–2249
32. Gabriel C, Peyman A, Grant EH (2009) Phys Med Biol 54:4863–4878
33. Sunaga T, Ikehira H, Furukawa S, Shinkai H, Kobayashi H, Matsumoto Y, Yoshitome E, Obata T, Tanada S, Murata H, Sasaki Y (2002) Phys Med Biol 47:N11–N15
34. Raicu V, Kitagawa N, Irimajiri A (2000) Phys Med Biol 45:L1–L4
35. Piskorowski J (2012) Measurement 45:1350–1361
36. Hejjel L (2004) Med Sci Monit 10:MT6–MT13
37. Fluhr JW, Gloor M, Lazzerini S, Kleesz P, Grieshaber R, Berardesca E (1999) Skin Res Technol 5:171–178
38. Mamishev AV, Sundara-Rajan K, Fumin Y, Yanqing D, Zahn M (2004) Proc IEEE 92:808–845
39. Leveque JL, Rigal JD (1983) J Cosmet Sci 34:419–428